JOURNAL OF THERMOPHYSICS AND HEAT TRANSFER
Vol. 17, No. 4, October–December 2003

Controlling Phase Interface Motion in Inverse Heat Transfer Problems with Solidification

R. Xu* and G. F. Naterer†
University of Manitoba, Winnipeg, Manitoba R3T 2N2, Canada

In this paper, an inverse numerical model is presented for solidification problems. It is used to predict the transient boundary conditions, which produce a prescribed interfacial surface motion and heat transfer. The formulation calculates the required boundary temperature to provide a specified velocity of the phase interface during solid–liquid phase transition. A control-volume-based finite element method is employed for the numerical solution of the energy conservation equation. The finite element framework provides a novel alternative to other inverse techniques based on structured grids. The effects of Stefan number and interface velocity on the solidification processes will be investigated. Numerical examples are presented and discussed for one-dimensional and two-dimensional solidification problems. The accuracy and performance of the formulation are assessed by comparisons with analytical solutions. Based on the model's capability of efficiently providing stable and accurate results, it is viewed to be a worthy design tool in practical engineering applications such as thermal energy storage and materials processing, such as casting and extrusion processes.

Nomenclature

c	=	specific heat
e	=	internal energy
k	=	thermal conductivity
L	=	latent heat
N	=	shape function
R	=	sensitivity coefficient in temperature calculation
S	=	source term
Ste	=	Stefan number
T	=	temperature
t	=	time
V	=	interface velocity
X_0	=	reference length
x, y	=	spatial coordinates
α	=	thermal diffusivity
Γ	=	thermophysical property
Δt	=	time step
ξ, η	=	local coordinates
ρ	=	density
Φ	=	general scalar variable

Subscripts

l	=	liquid
p	=	nodal point
$r, 0, w$	=	reference
s	=	solid

Superscript

m	=	iterative counter

Introduction

IN many industrial processes, effective thermal control involving phase change is required in a real-time mode to improve processing conditions. Thermal control has received considerable recent attention because of its wide practical applications. Specific examples include thermal control in materials processing, such as casting and molding, as well as ice accretion on structures. In materials processing applications controlling the heat transfer pattern is important because it can largely influence various processes, such as casting quality and production time. Demirci et al.[1] implemented this type of control successfully in molding processes. The heat fluxes and velocities of the solidification interface can be controlled in a manner such that specified casting/molding properties and structures of the material are achieved. For example, the processes can be controlled by utilizing measurements, such as thermocouple temperature measurements, during a process and then adjusting the external boundary conditions at a flow inlet in a real-time mode to give improved and desired results during solidification. Furthermore, Hale et al.[2] present an inverse methodology that permits independent control of the interfacial temperature gradient during a solidification process. These developments provide important progress in the development of advanced materials with improved mechanical properties.

The current control scheme requires a numerical simulation of the inverse heat transfer problem. Heat transfer can be classified as either a direct heat transfer problem or an inverse problem. In direct problems, certain initial and boundary conditions are given, such as specified temperature or heat-flux boundary conditions, and then distributions of the dependent variables, such as temperature, are obtained within the domain. Extensive research studies have examined direct problems in heat transfer with phase change. The methods for these problems, including analytical and numerical methods, have been well developed.[3]

On the other hand, the inverse heat transfer problem is concerned with the estimation of a required boundary heat flux, or temperature, based on internal measurements or a desired internal process behavior. It is well known that an inverse problem is much more difficult to solve numerically than a direct problem.[4]

The inverse heat transfer problem has been applied to two main areas: 1) the inverse heat-conduction problem (IHCP)[5–8] and 2) problems involving phase change.[9–13] In the inverse heat-conduction problem, the unknown boundary temperatures or heat fluxes are estimated by utilizing transient temperature measurements at one or more interior locations of the specified domain. This type of inverse problem has been the subject of considerable research. However, in the problems involving phase change, additional effects of phase change during solidification and melting problems provide further challenges in inverse modeling. In these problems, the temperature and the interface velocity can be prescribed at the phase interface. The required temperature and heat flux at the

Received 16 April 2002; revision received 26 March 2003; accepted for publiction 21 April 2003.

*Graduate Student, Department of Mechanical and Industrial Engineering.
†Associate Professor, Department of Mechanical and Industrial Engineering. Member AIAA.

stationary boundary of the domain are then unknown; these values must be determined by the numerical formulation. Because of the presence of a moving interface, the phase-change problem can become strongly nonlinear in the interfacial heat balance, and as a result there are only limited studies dealing with inverse heat-conduction problem involving phase change.

In this paper, a two-dimensional formulation of the inverse heat-conduction problem involving phase change will be examined. Several previous methods have been developed for the solution of this problem. In general, they can be categorized into the following overall groups: 1) analytical method, 2) front-fixing method, 3) front-tracking method, and 4) fixed domain method. There are only a limited number of analytical solutions available (mainly one-dimensional problems). In the front-fixing method and the front-tracking method, the solid and liquid regions are treated separately, and the phase-change interface is explicitly handled as a moving boundary. For the front-fixing method, the moving interface is fixed with an appropriate coordinate transformation, and the interface becomes effectively stationary. This method introduces numerical complications by the coordinate transformation. Zabaras[9] used a front-fixing method to obtain the solution of several one-dimensional inverse solidification problems. A finite element method with a future time-stepping technique was employed in this study. Front-tracking methods involve deforming and moving finite elements or finite difference grids. The mesh is continuously moving while adapting to the freezing interface motion.

Katz and Rubinsky[10] developed a front-tracking finite element method for the study of the inverse one-dimensional conduction heat transfer problem with phase change. Zabaras and coworkers[11,12] solved two-dimensional phase-change problems by a front-tracking method, and a boundary element analysis was used in conjunction with Beck's[5] sensitivity analysis. The solutions were stabilized at large time levels by a future time-stepping technique. This method offers the advantage of clearly separating the two phases along a boundary delineated by the mesh. However, the mathematical algorithms required to appropriately adjust the mesh are generally very complex. In many instances, this approach is computationally intensive and often difficult to implement in conventional schemes, such as finite element or finite volume techniques.

Fixed-domain methods[13] do not change the initial spatial discretization mesh. These methods involve the assumption of a continuous solid–liquid mixture (i.e., no internal gas voids). The problem is formulated in a way whereby the phase interface conditions become implicit within the conservation equations themselves (i.e., equations applied at interface and all other regions within fixed domain). Then, appropriate heat source terms (or effective specific heat in representation of latent heat) can be introduced, and a single differential equation is solved over the whole domain (solid and liquid). This method has the advantage of a single numerical implementation in both phases. Voller[13] introduced a method to solve the inverse one-dimensional Stefan problem based on an enthalpy formulation. The discretized inverse equations are obtained by a control volume approach and a time-stepping scheme. In this approach, the finite difference method is used, and the value of the liquid fraction can be used to track the progress of the solid–liquid phase interface. An iterative technique is adopted such that the solution provides a specified movement of the phase interface.

There are two commonly used techniques in fixed-domain methods, that is, effective specific heat technique and heat-source-term technique.[14] These two techniques define a total enthalpy H separately by an effective specific heat (effective specific heat technique) or a heat source term (heat-source-term technique) to account for the latent heat evolution in the governing energy equation. In comparison with the source-term technique, the effective specific heat technique often exhibits more stable behavior. In the source-term technique, source terms are often the cause of diverging iterations, particularly for problems with nonlinear source terms such as the solidification problem. In these problems, source-term linearization is necessary, and so a nonlinear latent heat relationship is expressed in an approximate linear form. As a result, achieving a converged solution depends on how well the source term is linearized. Also, when a source term is linearized such as $S = S_c + S_p T_p$ (in source-term linearization, S_c and S_p refer to the constant part of S and the coefficient of T_p respectively; T_p refers to the temperature at point p), the coefficient S_p must generally be negative.[15] In many cases, this is difficult to achieve, and divergence of the iterations occurs.

This paper will consider the numerical simulation of inverse phase-change heat transfer, during solidification and melting processes, by a control-volume-based finite element formulation. In this way, the model is conservation based while retaining the geometric flexibility of the finite element method. A fixed domain inverse method with an effective specific heat technique will be used, in both one-dimensional and two-dimensional solidification problems, such that the phase interface moves in a desired specified fashion. Some examples involving conduction with phase change will be presented. Also, the effects of Stefan number and interface velocity on solidification processes will be discussed. The preceding developments can provide important contributions in terms of control engineering for thermal problems involving solidification and melting in industrial processes.

Problem Formulation

In this paper, the governing equations will be written in a dimensionless form. We will define the following dimensionless variables,

$$\Gamma_k^* = \frac{\Gamma_k}{\Gamma_l} \tag{1}$$

$$V^* = \frac{V}{V_0} \tag{2}$$

$$T^* = \frac{T - T_w}{\Delta T_0} \tag{3}$$

$$e^* = \frac{e - e_w}{c_l \Delta T_0} \tag{4}$$

$$x^* = \frac{x}{X_0} \tag{5}$$

$$t^* = \frac{\alpha_l t}{{X_0}^2} \tag{6}$$

where the subscript k refers to phase (i.e., $k = 1, 2$ indicate solid and liquid phases, respectively). For the individual scalar fields, the reference scalar variables are

$$V_0 = \alpha_l / X_0 \tag{7}$$

$$\Delta T_0 = T_i - T_w \tag{8}$$

where T_i and T_w refer to reference temperatures; they can be taken as the maximum and minimum temperatures, respectively. Unlike direct problems with Dirichlet boundary conditions, the temperature nondimensionalization in inverse problems involves boundary temperatures that vary in time. Thus, the selected characteristic reference temperatures might not be the maximum and minimum temperature throughout the problem. In subsequent governing equations all variables will be written in a dimensionless form without the superscripts* (removed for brevity).

The governing equation for two-dimensional, diffusion-dominated energy transport with solid–liquid phase transition (pure material) can be obtained by applying the principle of conservation of energy to a specified control volume located at a given position in the domain. The energy conservation equation can then be written as

$$\frac{\partial}{\partial t}(\rho e) = \nabla \cdot (k \nabla T) \tag{9}$$

An equation of state is required in order to write the energy equation in terms of temperature alone. In the present work, a piecewise linear

equation of state will be expressed in one equation (where subscripts $k = 1, 2$ refer to solid and liquid phases, respectively) as

$$e = e_{r,k}(T) + c_{r,k}(T)(T - T_{r,k}) \tag{10}$$

The reference values can be obtained by integration of the Gibbs equation from a point in the liquid region to another point in the solid region. In this way, both latent and sensible heat contribution sappear in the energy distribution. These variables have been consistently set to the following values.

($k = 1$, solid phase):

$$e_{r,1} = 0 \tag{11}$$

$$T_{r,1} = 0 \tag{12}$$

$$c_{r,1} = c_s/c_l \tag{13}$$

($k = 2$, liquid phase):

$$e_{r,2} = (\bar{c}/c_l)(T_l - T_s) + (c_s/c_l)(T_s) + 1/Ste \tag{14}$$

$$T_{r,2} = T_l \tag{15}$$

$$c_{r,2} = 1 \tag{16}$$

where $\bar{c} = \frac{1}{2}(c_s + c_l)$, $Ste = c_l \Delta T_0/L$, and T_s and T_l represent the solidus and liquid temperatures, respectively (Fig. 1). For a pure material, $T_s = T_l = T_m$ (T_m refers to melting temperature). However, $T_s < T_l$ for multicomponent systems. In the solid phase, the reference temperature is selected to be the minimum temperature T_w, thereby making $T_{r,1} = 0$, based on the nondimensionalization described in Eq. (3). In the liquid phase, the minimum temperature encountered is $T_l = T_m$, which is thus used as the reference temperature, $T_{r,2}$, in that phase. In this approach (called the "effective specific heat" technique, rather than "source-based" approach) the latent heat arises through the preceding $1/Ste$ term because phase transition requires an energy change corresponding to the latent heat of fusion (represented within Stefan number).

In addition, the formulation of the phase-change problem requires appropriate boundary and initial conditions. Spatial boundary conditions in direct heat transfer problems are generally classified into three main types: 1) Dirichlet conditions (specified value of surface temperature), 2) Neumann conditions (specified value of outward normal heat flux/temperature gradient), and 3) Robin conditions (convection condition).

For the inverse problem, with the exception of the boundary where the temperature will be controlled, all boundary conditions can be treated in a similar way as direct problems (Dirichlet, Neumann, and Robin boundary conditions). However, at the controlling boundary the temperatures are unknown, and they represent the solutions of the inverse problem. A temperature at this boundary is obtained by iterations following an initial estimate; in other words, at the beginning of each time step, an estimated temperature is initially given. Usually, it is set equal to the temperature from the previous time step. During each time step in the solution, the controlling boundary temperature (at $x = 0$ in our case) is updated at each iteration until the predicted movement of the interface agrees, within a given tolerance (10^{-4} in this paper), with the specified (or desired) movement. The update used in this work is given by

$$T_0^{m+1} = T_0^m + \left(T_p^{m+1} - T_p^m\right)/R_p \tag{17}$$

where m is the iterative counter (within a given time step) and the subscript 0 refers to boundary nodal point. For the current time step, the specified interface position is at an interior nodal point p. The updated boundary temperature in each iteration is then based on the boundary temperature from the last iteration, the temperature difference at the interior nodal point p between previous and current iterations, and the sensitivity coefficient. In a one-dimensional case, the single boundary temperature is updated by using information from the specified interface position (the single interior nodal point p). For two-dimensional problems, such as the two-dimensional example involving aluminum (upcoming section), the boundary temperatures at multiple points need to be predicted. When using Eq. (17) to update boundary temperatures during the iterations, boundary nodal points are associated with interior nodal points, which are along the same row. In other words, the interior nodal point p is located along the same row, which is projected inwards from boundary nodal point 0. Because the interface position at nodal point p is only used to update T_0 at the boundary in the same row, then the boundary temperature on another row does not directly influence the temperature at that node. Following each update, the two-dimensional heat equation is solved throughout the domain, and convergence is achieved when the interface temperature sufficiently matches the phase-change temperature. Thus, the two-dimensional effects are experienced when the full two-dimensional heat equation is solved, rather than interrow effects in the boundary temperature updates. In relation to the uniqueness question, if temperatures along different rows were involved in the boundary temperature updates, then this might affect the convergence performance. However, the procedure would still solve the two-dimensional heat equation to reach convergence, so that the same answer would be obtained as without the interrow updating. Thus, there is only one unique solution in either scenario.

Since the problem is transient (i.e., dependent variables change with time), initial conditions are also required in order to give the distribution of the temperature within the entire region at the initial state ($t = 0$).

Numerical Procedure

A control-volume-based finite element method is used in this paper to solve the governing equations and implement the inverse method in the numerical procedure. In comparison with conventional finite difference methods, a finite element approach has more geometric flexibility for applications to two- or three-dimensional problems. Currently, a finite volume is defined and divided into a set of subvolumes with finite element nodes distributed throughout the domain. A two-dimensional domain and linear, four-noded quadrilateral elements are used. Figure 2 shows a typical control volume that is divided into four sub-control-volumes (SCV) associated with a particular node. The boundaries of sub-control-volumes will be called subsurfaces. Additional details of the finite element

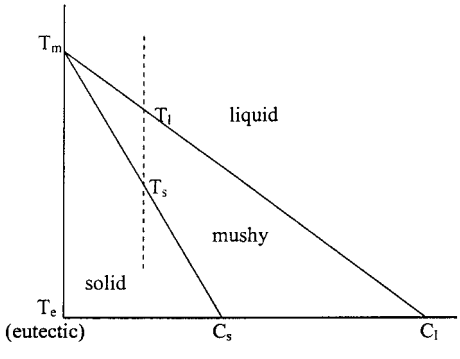

Fig. 1 Binary alloy phase diagram.

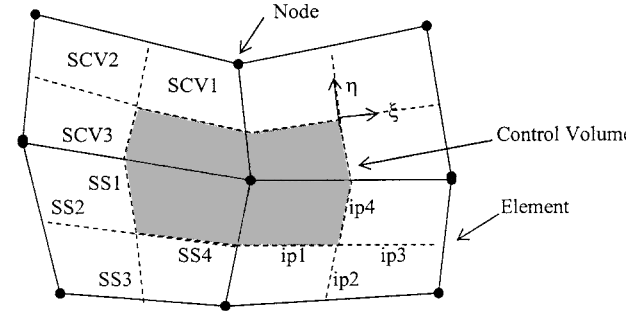

Fig. 2 Element and control volume.

discretization, in relation to direct problems, are available in Ref. 16. The focus of the current paper is the development of an inverse procedure in the control-volume-based finite element framework. In this way the inverse algorithm will be conservation based, while retaining the geometric flexibility of finite elements.

A Crank–Nicolson scheme is used to evaluate diffusion and source terms at the intermediate time level. In particular, this intermediate time level refers to the midpoint between the current time level and preceding time level. For example, if we let the superscripts $n+1$ and n refer to current and preceding time step, then the diffusion flux (x component) in Eq. (9) is evaluated as

$$\boldsymbol{F}_x^d\big|_{\text{ip}} = k \sum_{i=1}^{4} \frac{\partial N_i}{\partial x} \left(\frac{T_i^{n+1} + T_i^n}{2} \right) \tag{18}$$

and similarly in the y direction. The coefficients at step $n+1$ remain as active coefficients in the implicit solution, whereas terms at step n (i.e., lagged terms) are grouped together into the source term. The overall algorithm then becomes second-order accurate in time. Also, the spatial discretization provides essentially second-order accuracy in space.[16]

In the inverse problem, the governing equations are identical to the equations in the corresponding direct problem. The difference arises because the interface position is given, instead of unknown, and the temperatures at the controlling boundary are unknown, rather than boundary conditions. The other boundary conditions are given as the same conditions arising from the direct problem. We have an interface that moves across one grid spacing at each time step during the simulation. Given the movement of the interface (i.e., prescribed velocity of the interface), we then select a constant time step. During the calculations, a node-jumping method is used, whereby at any time step the interface moves from one node point to the next adjacent point. Therefore, a fixed numerical grid is specified according to prescribed interface velocity and time step. The grid can be uniform (constant interface velocity) or nonuniform (variable interface velocity) according to the different specified interface velocities in a particular inverse problem. Initially, during each time step, a tentative (estimated) temperature at the controlling boundary is used, and the equations are solved like a direct problem. In this paper, the temperature at the preceding time step was adopted as the tentative temperature. The desired interface motion was specified by the properties and the reference values in Eqs. (11–16) at each node point. The temperatures at the controlling boundary are then updated continuously using Eq. (17) in an iterative manner until the predicted movement of the phase interface agrees within a given tolerance (10^{-4} in this paper) with the desired path. In a one-dimensional case, the temperature at the single boundary nodal point is updated at each iteration. By solving the governing equation, we obtain the entire temperature distribution throughout the domain. Then, we check the temperature at the desired interface position to decide if the solution at the given time step is completed. In other words, if the temperatures at the desired interface position agree with the phase-change temperature within a given tolerance, we stop iterating in the current time step and start the next time step. Otherwise, we continue to perform iterations. In the one-dimensional case, the interface is at a single nodal point, and the temperature at this point is used to determine if the calculation converges. In a two-dimensional case (such as two-dimensional aluminum solidification in next section), there are multiple points on the phase interface. In this study, we use the midpoint to check if the temperature converges to the phase-change temperature because the desired interface motion is specified indirectly by a node-jumping method as just mentioned (i.e., specify the properties and the reference values at each node point for the desired interface motion).

Furthermore, a sensitivity coefficient will be defined as follows:

$$R_p = \frac{\partial T_p}{\partial T_0} \tag{19}$$

where the subscript 0 refers to boundary. This coefficient essentially measures the influence of changes in the boundary temperature T_0 on the temperature at the point p (inside domain). The range of sensitivity coefficient R lies between 0 and 1. The value of R expresses the effective temperature connection between the point p and the controlling boundary. As the sensitivity coefficient R becomes larger, then the influence of the changes in the boundary temperature on the temperature at point p becomes stronger. It is apparent that as a point lies closer to the controlling boundary, the sensitivity coefficient becomes larger. This coefficient will be used to update the boundary temperature in the current inverse method.

Furthermore, if we write T_p^{m+1} in terms of a Taylor-series expansion, it can be expressed as

$$T_p^{m+1} = T_p^m + \frac{\partial T_p}{\partial T_0}\left(T_0^{m+1} - T_0^m\right) + \frac{1}{2!}\frac{\partial^2 T_p}{\partial T_0^2}\left(T_0^{m+1} - T_0^m\right)^2 + \cdots\cdots \tag{20}$$

Neglecting higher-order terms (only first two terms retained) and rearranging Eq. (20), then it becomes evident that Eq. (20) becomes equivalent to the boundary temperature equation described earlier in Eq. (17).

We will now consider how to perform effectively the numerical calculation of the sensitivity coefficient. Substituting Eq. (10) into Eq. (9), we find that the heat-conduction equation becomes an equation in terms of temperature alone. Then, taking derivatives with respect to T_0 on both sides of the equation, we obtain a resulting equation in terms of the sensitivity coefficient R. The resulting equations can be written in the following form:

$$\left(\frac{\rho J_1}{\Delta t}\right) R_p^{n+1} = \left(\frac{\rho J_1}{\Delta t}\right) R_p^n + \frac{1}{2} \sum_{i=1}^{4} \int_{S_i} \boldsymbol{F}^r \cdot \mathrm{d}\boldsymbol{n}|^{n+1/2} + \bar{S}_T \tag{21}$$

where J_1 refers to SCV area. Also,

$$\boldsymbol{F}_j^r(R_i)|_{ip} = k \sum_{i=1}^{4} \frac{\partial N_i}{\partial x_j} R_i \tag{22}$$

$$\bar{S}_T = \frac{1}{2} \sum_{i=1}^{4} \int_{S_i} \boldsymbol{F}^r \cdot \mathrm{d}\boldsymbol{n}|^n \tag{23}$$

Furthermore, the boundary condition for sensitivity coefficient is given by

$$R_0{}^k = 1, \qquad k > 0 \tag{24}$$

and for the initial condition by

$$R_p{}^0 = 0, \qquad \text{all} \quad p \tag{25}$$

where the subscript denotes nodal point and the superscript denotes time level. By a similar procedure as the solution of the direct problem, the resulting equations can be solved numerically and the solutions R at each point can be obtained.

It should be emphasized that the resulting finite volume equation for R_p in Eq. (21) is solved with the finite element method [based on the control-volume finite element method (CVFEM)]. Thus, each nodal R_p is determined from a finite element equation developed locally within each element, rather than globally and dependent on the nearby mesh configuration. In this sense of a finite element framework, the method is considered to be applicable to unstructured grids because the local elemental equations are developed independently of the nearby node numbering. The internode connectivity is handled independently, when the assembly of all elements is completed.

The numerical procedure for the inverse solution can now be summarized as follows:

1) Specify the movement of the phase interface (i.e., interface velocity), and choose a constant time step based on this interface velocity.

2) Based on the velocity of the interface and the chosen time step, then a fixed numerical grid is specified, such that at any time step the interface moves from one grid point to the next grid point. If a variable interface velocity is specified, then either a variable time step, or nonuniform grid, is selected. In this work, the latter approach is adopted.

3) Within each time step, an estimate of the unknown controlling boundary temperature is given (equal to the temperature from the preceding time step), and then the energy equation is solved in a direct manner for the temperature T.

4) The sensitivity coefficients [Eq. (19)] are obtained, and the unknown (controlling) boundary temperature is updated. Then, the energy equation is solved again.

5) Repeat steps 3 and 4 for each iteration in solving the energy equation. The solution is terminated when the predicted movement of the interface agrees, within a given tolerance, with the specified (desired) interface movement.

At some stage, as the interface moves further and further away from the controlling boundary, the sensitivity coefficient becomes smaller, and the iterative updating of the boundary temperature becomes more difficult. If numerical instabilities arise in the preceding procedure, that is, oscillations with diverging solutions within iterations, then the current approach in handling this situation is further grid refinement. Alternatively, a smaller time step can be selected. Further stability measures based on entropy techniques are described in Ref. 17.

Although the phase interface motion is controlled by surface temperature in this paper, the method can be applied to other boundary variables of heat flux or heat transfer coefficient. If the surface temperature cannot be controlled practically, only one additional step is needed in the numerical simulation to calculate the required surface heat flux, instead of the surface temperature.

In the following section we will consider applications of the current formulation to two example problems with phase change.

Results and Discussion

Numerical results will now be presented for illustration of some general features, performance, and accuracy of the proposed inverse methodology. Each example involves a solution for the boundary temperature, which produces a prescribed moving phase interface shape and motion. The following problems will be considered: 1) one-dimensional solidification with constant interface velocity and 2) two-dimensional solidification involving pure aluminum. The finite element program is validated through comparisons with results from available analytical solutions.

In many inverse heat-conduction problems, real sensor measurements from one or more interior locations of the domain are used to predict the unknown boundary temperatures.[8] In such cases, any "noise" in the system can seriously affect the stability of the inverse algorithm employed. However, in the following problems, the movement of the phase interface is prescribed. During each time step, the iterations converge until the temperature at the desired interface position is equal to the phase change temperature. Because we have specified the moving interface position, the interface temperature provides an error-free value equal to the phase change temperature. As a result, the effects of noise on the stability of the algorithm are not examined in detail here. Numerical simulations were performed with a Pentium 233-MHz computer, and the solution at each time step generally required only a few seconds. The fast simulations indicate the efficient performance of the current procedure and its potential for applications in a real-time control mode.

One-Dimensional Solidification with Constant Interface Velocity

By considering the following solidification process, involving a pure material, we can examine the possibility of implementing the inverse method in a practical application. An enclosure (see Fig. 3) is initially occupied by a pure liquid at a temperature of T_{in}, and T_m denotes the melting (phase change) temperature. The top, bottom, and right walls are insulated, and no temperature gradients are initially present in the liquid region. The liquid is initially at melting temperature T_m. The position of the interface will be mainly controlled by the temperature at the left boundary of the cavity. The conductivity k, density ρ, and specific heat c are assumed to be independent of temperature. Also, it is assumed that the interface moves in the x direction and the shape of the interface is linear and vertical (at all time levels) and the velocity of the interface is constant. We will solve this problem to assess how the temperature at the left boundary should vary with time to produce the desired interface motion. In this example, the temperature at the left boundary will be uniform, and it will only change with time, that is, $T_0(t)$. It can be treated as a one-dimensional heat transfer problem, although the discretized domain and numerical formulation will be given in a two-dimensional framework. The temperature at the left boundary will be predicted by the current inverse method in order to control the interface shape (linear) and motion (velocity) during solidification. This problem is based on examples considered earlier by Voller[13] and Zabaras et al.,[12] except that an extended range of Stefan number and interface velocities are presented herein. The following problem parameters (dimensionless) are adopted in this example:

$$\alpha = 1, \qquad c = 1$$

This problem was chosen as a validation problem because an analytical solution is readily available. At $x = 0$, the solution for the surface temperature required to produce the prescribed motion (constant interface velocity) is reported by Carslaw and Jaeger[18] as (in dimensionless form)

$$T(0, t) = T_0 + (1/Ste)\{1 - \exp[(V^2/\alpha)t]\} \tag{26}$$

Computed results will be compared with this exact solution. In the numerical solution, since the interface is required to move at a constant velocity, a constant time step and uniform grid are adopted. The discussion here will be largely focused on the effects of Stefan number and interface velocity on the inverse computations. All variables in the following figures are dimensionless as defined earlier in the problem formulation section. For example, $T^* = (T - T_w)/(T_i - T_w)$. In this example the reference temperatures were taken as $T_i = 1°\text{C}$ and $T_w = 0°\text{C}$ (not the maximum and minimum temperatures in the domain in this example). The variables T_i and T_w represent the reference temperatures, and they were used for purposes of nondimensionalization in Eq. (3). Figure 4 shows the effects of Stefan number on the solidification process. The figure illustrates how the required boundary temperatures vary

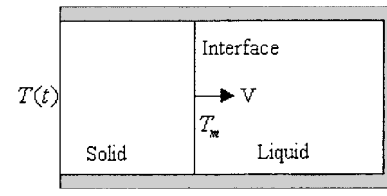

Fig. 3 One-dimensional inverse solidification problem.

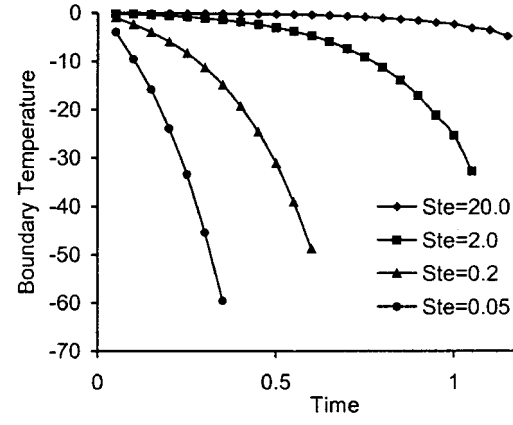

Fig. 4 Boundary temperature for different Stefan number.

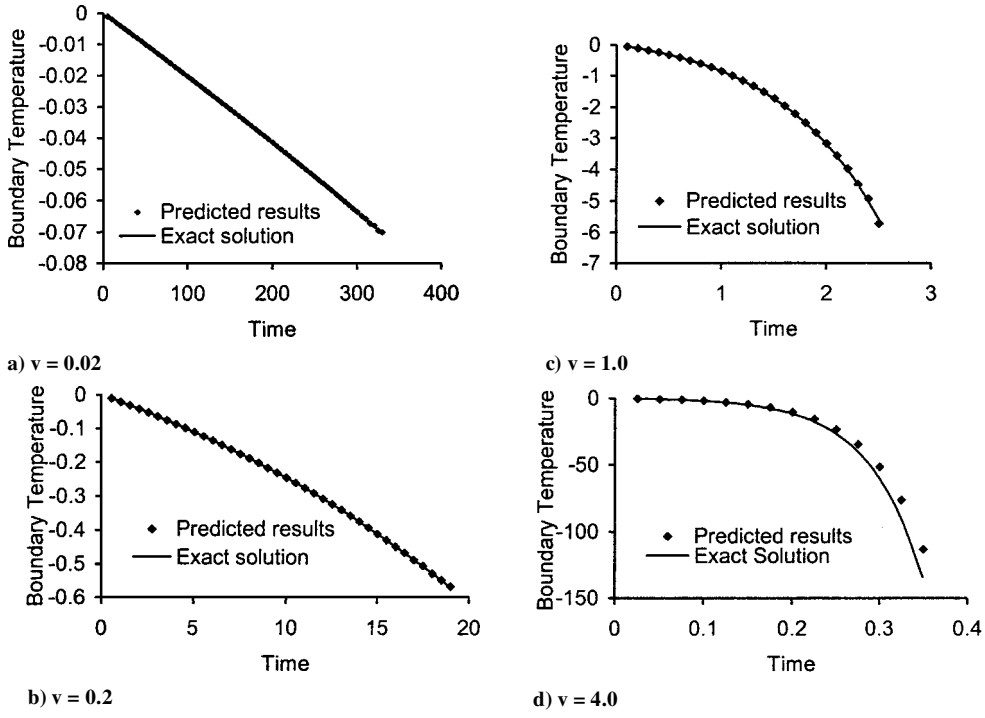

Fig. 5 Boundary temperature for different interface velocities.

with time for different Stefan numbers, that is, $Ste = 0.05$, 0.2, 2, 20, respectively. During the calculations for different values of Stefan number, the same time step and same interface velocity were taken ($\Delta t = 0.05$, $V = 2$). From Fig. 4, for each Stefan number, the required boundary temperatures (to ensure $V = 2$) decrease with time. As the Stefan number becomes smaller, the required boundary temperature decreases more quickly to achieve the same interface velocity. In other words, as the Stefan number decreases, a lower boundary temperature is required. This result was expected because a lower Stefan number represents a material with a higher latent heat of fusion. A material with a lower Stefan number releases/absorbs more energy as it undergoes phase change. Therefore, lower boundary temperatures are required to sufficiently cool the material at lower Stefan-number values. In some cases, if the Stefan number is very small and the interface is specified to reach a certain velocity, it might be impossible in practice to ensure that the boundary temperature decreases sufficiently fast. If a solidification process involving a material with a small Stefan number has to provide a certain interface velocity and material quality, some consideration can be given to changing the material's properties by adding other alloy constituents into the material.

Additional effects of interface velocity on the solidification processes were investigated, and the results are shown in Fig. 5. The Stefan number ($Ste = 2.0$) and grid configurations were maintained as identical in these cases. The time steps were changed based on the different interface velocities. Figures 5a–5d reveal that the required boundary temperatures vary as a function of time for different interface velocities ($V = 0.02$, 0.2, 1.0, 4.0). As expected, a larger interface velocity requires that the boundary temperature decreases much faster than cases involving a smaller interface velocity. Also, the exact solutions for different situations are given in order to compare the present results with the exact solutions. Figures 5a–5d show that the numerical computation gives generally accurate results at small values of V, but the accuracy of the predictions is somewhat reduced with faster interface movement. For example, at an interface velocity of 0.02, the predicted results agree well with the exact solution. As the interface velocity increases to 4.0, the accuracy of the numerical computations in terms of required boundary temperature is reduced by 5%.

Also, the accuracy of the numerical computations can be improved by refining the grid and the time step. A given interface

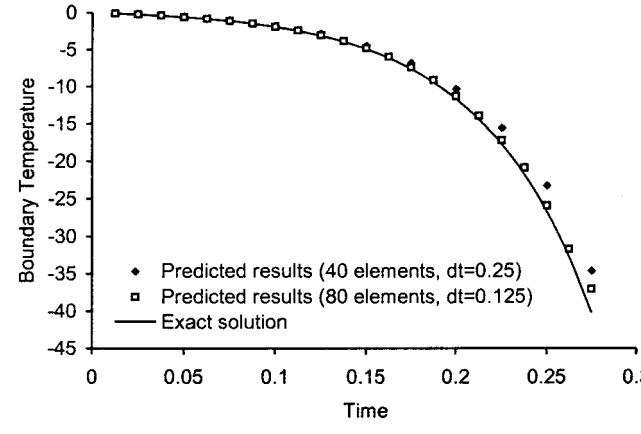

Fig. 6 Boundary temperature for different grid refinements.

velocity ($V = 4.0$) is specified, and so the problem remains identical after refinement of the grid spacing and time-step size. Figure 6 indicates that the solution accuracy is improved when the number of grid points is doubled.

As the interface velocity decreases, the numerical computations remain stable over a larger number of time steps. For example, at $V = 0.02$, more than 60 steps of time advance are predicted well, but fewer steps retain stable computations at higher interface velocities. In some sense this trend arises partly from the impractical nature of the required exponential decrease of boundary temperature in Eq. (26). This exponential decline would be difficult to achieve in practical applications because $T_0(t)$ must eventually become infinitely low at $x = 0$, particularly for high values of V. However, it does represent an effective benchmark problem for model validation, as well as practical circumstances at early stages of typical solidification applications.

The program is executed on a personal computer, and computations generally require only a few seconds for convergence within each time step. If we compare execution time in the program with the actual (physical) time step in practice, then the physical timescale is substantially larger than the computational timescale. Thus, it is feasible to apply the program in a practical control setting for

solidification processes. In other words, since the computational time required to advance the phase interface a given distance is more than an order of magnitude less than the physical time in the interface advance, it appears that the algorithm might be suitable for a real-time control setting.

The results from the thermal predictions can allow a control engineer to modify the boundary temperature in time to have the desired interface movement in a given time increment. In more complicated problems, such as three-dimensional predictions with fluid flow, it is likely that the computational time might exceed the corresponding physical time. For example, the CPU time taken over a time step in the numerical simulation would exceed the actual time required. However, with the rapid advance of computing technology and processor speed it is anticipated that control engineering, merged with computational fluid dynamics (CFD), will become a viable alternative to conventional control techniques. For example, recent studies involving the NASA Lewis Research Center[19] have facilitated the use of CFD by control engineers designing propulsion controls.

Two-Dimensional Solidification with Pure Aluminum

Metal solidification of quadrilateral-shaped objects is often encountered in industrial applications. Examples include feeder systems in casting-mold assemblies and extruded parts. But in the present problem, the domain characterizes spokes in a rotor support (see Fig. 7). A benefit of the carefully controlled solidification process is to ensure alignment of the grain boundaries in a predetermined direction for highest resistance to thermal and other stresses encountered by the component during operation. Under certain operating conditions the highest stresses would be best resisted when the spoke is cooled in the direction parallel to the spoke face because of the resulting alignment of grain boundaries.

We will consider solidification in a region (see Fig. 8) occupied initially by pure aluminium at the melting temperature T_m (i.e., slight undercooling required, below T_m for onset of solidification). The top, bottom, and right boundaries of the cavity are adiabatic. The conductivity k, density ρ, and specific heat c are assumed to be independent of temperature. It is desired that the interface velocity varies with height y, so that the shape of the interface remains approximately linear, and all points on the interface reach the right boundary at about the same time. In this way, the resulting grain boundaries can be aligned in a manner that

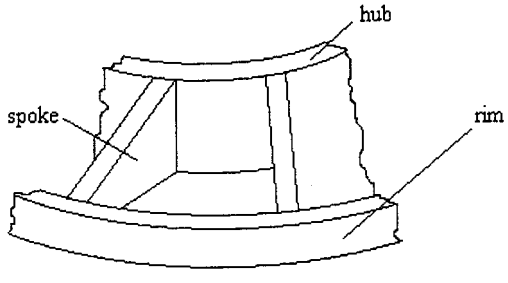

Fig. 7 Quadrilateral-shaped section of rotor support casting.

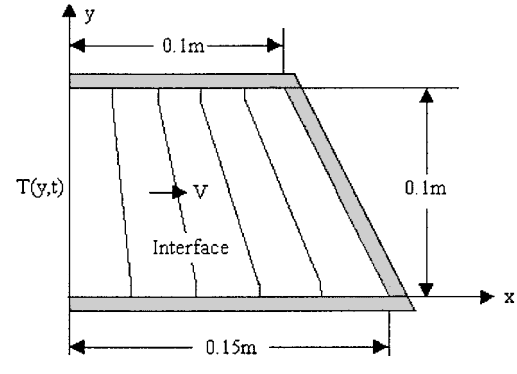

Fig. 8 Two-dimensional inverse solidification problem.

Table 1 Thermal properties of pure aluminum

Problem parameters	Value
Specific heat in liquid, c_l	1056.88 J/kg°C
Specific heat in solid, c_s	1056.88 J/kg°C
Heat conductivity in liquid, k_l	229.28 W/m°C
Heat conductivity in solid, k_s	229.28 W/m°C
Diffusivity in solid, α_s	$8.1865 * 10^{-5}$ m^2/s
Diffusivity in liquid, α_l	$8.1865 * 10^{-5}$ m^2/s
Density, ρ	2650 kg/m^3
Latent heat, L	397,480 J/kg
Reference length, X_0	0.1 m
Time step, Δt	125.0 s
Melting temperature, T_m	660 °C

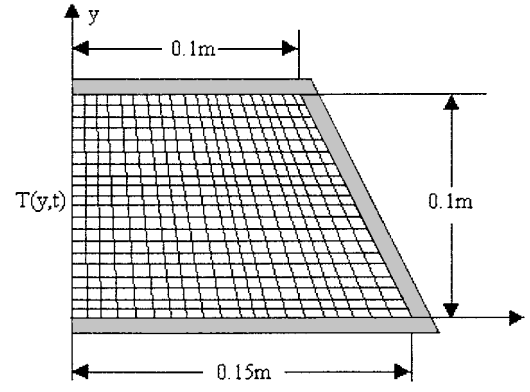

Fig. 9 Mesh structure.

allows the final solidified component to effectively resist conditions of high stress. The position of the interface will be controlled by the temperature along the left boundary of the cavity. We will solve this problem in order to obtain the manner in which the temperature at the left boundary should vary with time t and position y, that is, $T_0(t, y)$.

In practical applications, it might be difficult to implement such predictions exactly as the numerical simulation required. The method can be applied for interface control by dividing the surface into certain zones and then controlling the temperature or heat flux over the zones. Then, a mean or average predicted temperature or heat flux within the zones can be used, so the resulting conditions would come as close as possible to the desired result. Errors in discretizing the regions into such zones could be reduced when the number of the zones increases. Although it might be difficult in practise to obtain results exactly as desired, the current approach strives to improve the quality of solidified materials by applying a deterministic control of temperature or heat flux at the surface. This example is a fully two-dimensional problem. The thermophysical parameters in this simulation are shown in Table 1.

Figure 9 shows an outline of the mesh structure for the finite element discretization. The simulation is performed with a 20×20 mesh. The results for the top, midpoint, and bottom boundary temperature are shown in Fig. 10. Although no exact solution is available for direct comparisons, we can still compare the temperature at the midpoint of the left boundary to the average of a similar one-dimensional problem. An equivalent one-dimensional problem refers to heat transfer with phase change along the horizontal midplane of a two-dimensional rectangular domain having the same width as the original midplane. Meanwhile, Fig. 11 shows the results for the distribution of temperature at the left boundary at different times, and the trend of temperature appears qualitatively correct. In particular, the average left boundary temperature decreases with time, and the temperatures along the left boundary increase from the bottom to the top boundary.

Also, we have compared the temperature for a point at the left boundary with the analytical solution of the equivalent one-dimensional problem at the top and found that the temperature is

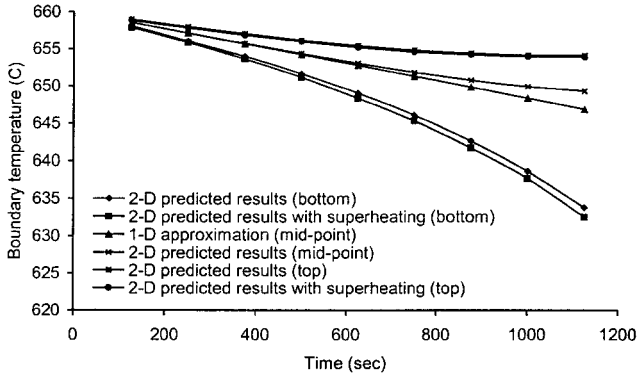

Fig. 10 Boundary temperature at midpoint, top, and bottom for solidification of pure aluminum.

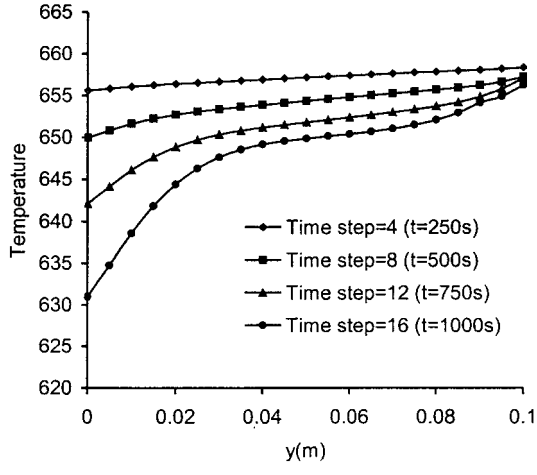

Fig. 11 Boundary temperature for solidification of pure aluminum.

higher than the analytical solution, whereas at the bottom the temperature is lower than the analytical solution. This reveals the proper trends of the two-dimensional effects in this problem. Heat transfer occurs from the top to the bottom regions. Thus, at the top, the boundary temperature does not need such a cold value as the one-dimensional problem. At the bottom, the boundary temperature should be colder than the temperature in the equivalent one-dimensional problem. The results appear feasible in this application problem. Because the focus of this work is conduction-dominated phase change, appreciable superheating in the liquid generates free convection in the liquid and interfacial regions, which is beyond the scope of the present inverse study. Figure 10 shows the effects of liquid superheating on boundary temperature at the top and bottom at a low level (2°C above the melting temperature) when free convective effects can be neglected. We found the boundary temperatures are lower than the case without superheating. Certain success with inverse phase change and free convection has been reported.[20] Also, ongoing studies are further confirming the suitability and performance of the current methodology in inverse convection/phase change problems.

In the preceding results, identical properties for the liquid and the solid were used. However, this is generally not the case in practice. It is necessary to examine how different properties in the solid and the liquid affect the results. Figure 12 shows the results for midpoint boundary temperature under the influence of different conductivities k for the liquid and the solid. Here, we define $R1$ as a ratio of conductivity between the solid and the liquid ($R1 = k_s/k_l$). The cases for $R1 = 1.0, 1.2, 1.5$ were examined separately because the conductivity of the solid is typically larger than the conductivity of the liquid for aluminum. It can be observed that higher conductivities in the solid lead to a slower decline of boundary temperature. As expected, a lower temperature gradient at the wall is sufficient to yield the same rate of heat extraction when the solid conductivity is

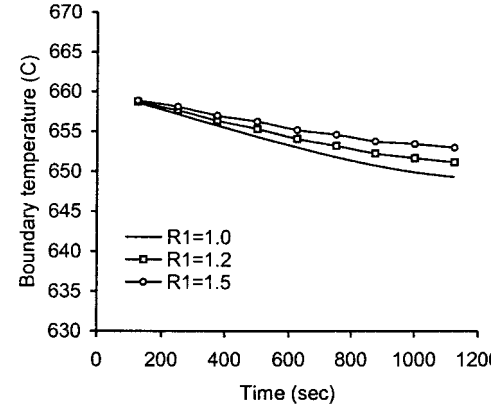

Fig. 12 Boundary temperature at midpoint for different $R1$ and pure aluminum ($R1 = k_s/k_l$).

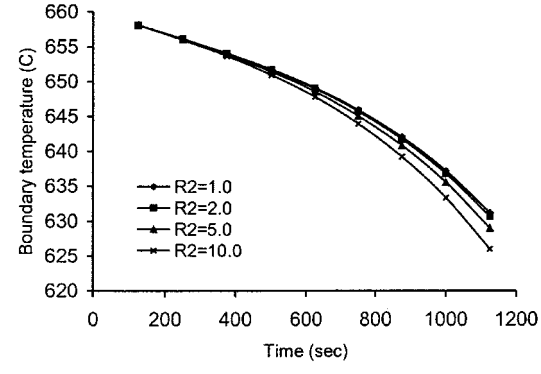

Fig. 13 Boundary temperature at the bottom for different $R2$ for pure aluminium ($R2 = c_s/c_l$).

higher. Figure 13 shows the results for the bottom boundary temperature under the influence of different specific heats c for the liquid and the solid. We defined $R2$ as a ratio of specific heat between the solid and the liquid ($R2 = c_s/c_l$). The cases for $R2 = 1.0, 2.0, 5.0, 10.0$ were examined separately. In Fig. 13, it can be observed that the boundary temperature at the bottom is lower at a particular point in time when $R2$ is higher (where $R2 = c_s/c_l$). If a higher $R2$ is interpreted as a lower c_l while keeping c_s constant, then this represents a lower Stefan number because $Ste = c_l \Delta T_0 / L$. Then, a lower boundary temperature at lower Stefan numbers appears consistent with results obtained earlier in Fig. 4.

Furthermore, the grid structure (see Fig. 9) indicates that the current inverse methodology has been successfully applied to grid discretizations involving skewed elements. It is possible to propagate a curved phase interface across a rectangular domain. Because the phase interface boundaries at each time step are known (specified or desired) in the inverse problem, the mesh can be generated in accordance with that motion. Because of the flexibility of such mesh generation, the method has generality in solving problems involving curved interface motion.

When compared to other conservation-based methods for inverse phase change (i.e., Voller[13,14]), it also exhibits greater generality because the local finite element equations are developed independently of the mesh configuration. Thus, only modifications of the mesh file are needed for different geometrical configurations, rather than code redevelopment when internal node equations are dependent on the mesh configuration. The focus of the current work is to demonstrate a useful CVFEM alternative to conventional methods, rather than claiming to handle highly complex two-dimensional problems. Despite the limitations of the current method to node jumping and interface propagation along lines (as commonly handled by other conventional methods) it still represents useful contributions to the literature through its CVFEM approach and treatment of sensitivity coefficients therein.

Table 2 Summary of capabilities of various inverse methods

Capability	Ref. 20	Ref. 10	Ref. 21	Ref. 22	Ref. 8	Ref. 23	Ref. 24	Ref. 13	Ref. 25	Ref. 26	Ref. 27	Ref. 28	Ref. 29	Ref. 30	Ref. 17
One-dimensional	X	X	X	X	X	X	X	X	X	X	X	X	X	X	X
Two-dimensional	——	——	X	X	X	X	X	——	——	X	X	——	——	X	X
Conduction	X	X	X	X	X	X	X	X	X	X	X	X	X	X	X
Fluid flow	——	——	——	X	——	——	——	——	——	——	X	——	——	X	——
Phase change	——	X	——	——	——	——	——	X	——	X	——	X	——	X	X
Conservation based	——	——	——	X	X	——	——	X	——	——	X	——	——	X	X
Structured grids	X	X	X	X	X	X	X	X	X	X	X	X	X	X	X
Unstructured grids	X	X	X	——	——	——	——	——	X	X	——	X	X	X	X
Skewed elements	——	——	——	——	X	——	——	——	——	X	——	——	——	X	X
Fixed domain	X	——	X	X	X	X	X	X	X	——	X	——	X	X	X
Interface tracking	——	X	——	——	——	X	X	——	——	X	——	X	——	——	——
Source based	——	X	——	X	——	——	——	X	——	——	X	——	——	——	——
Heat capacity based	——	——	——	——	——	——	——	——	——	——	——	——	——	X	X

At this stage it is worthwhile to summarize the contributions of the present work and place it within the context of other similar studies.[8,10,13,17,20–30] This summary is provided in tabular form (see Table 2) to clearly distinguish the features, capabilities, and limitations of other predictive models. An X designation in a box indicates that the reported results (cited researchers shown in references) exhibit the capability or characteristic listed in that particular row. It should be emphasized that a missing X might refer to "not a feature" or "not applicable," that is, algorithm different than conventional methods listed. Some rows refer to type of formulation (i.e., source based), whereas other rows refer to specific desirable characteristics of the method (i.e., two dimensional as well as one dimensional).

The terminology in Table 1 can be explained as follows: "Conservation based" refers to a control volume approach so that the problem scalars are conserved by direct enforcement of discrete conservation laws (desirable feature). Finite differences suggest "structured grids," whereas finite elements permit "unstructured grids" (desirable, as it allows complete geometric flexibility). "Skewed elements" (desirable capability) indicates whether the reported study demonstrates this feature. "Fixed domain" and "interface tracking" (i.e., front tracking, fixing, as described in Introduction), as well as "source based" (latent heat source terms) and "heat capacity based" (modified specific heat containing latent heat), refer to methods dealing with phase-change problems.

This paper uses an enthalpy-based method, with an effective specific heat rather than a source-based approach (as used by other standard inverse methods, i.e., Voller,[13,14]), to solve inverse phase-change problems. In this way it is viewed that less restrictive mesh and time-step requirements are apparent than other previously described methods because wide source term variations with Stefan number can destabilize the numerical solution. When compared to previous work of others, another useful aspect is the CVFEM for solving the governing equations. This formulation is conservation based, and each discrete equation is developed at an elemental level, independent of the mesh configuration. Also, unlike previous first-order methods in time, a Crank–Nicolson scheme was developed and applied to the diffusion and source terms at the intermediate time level. This improves the overall temporal accuracy of the inverse method to second-order accuracy in time. Larger time steps can be used while still maintaining numerical stability in the solutions. Overall, it is worthwhile observing that the currently reported model provides a contribution to inverse method development in view of its ability to simultaneously combine most desirable capabilities of other models into a single formulation, thereby yielding a flexible, efficient, and accurate tool for design purposes.

Conclusions

An enthalpy method, with an effective specific heat and a finite element formulation, has been employed for simulations of one-dimensional and two-dimensional inverse solidification problems involving specified phase interface velocities. The enthalpy method is based on a node-jumping algorithm, which calculates the boundary temperature for a given interface velocity. The finite element formulation permits flexibility in inverse problems with irregular geometries, and the finite volume discretization provides conservation-based properties in the overall scheme. The solutions from two validation problems indicate favourable agreement with other available solutions. Also, the results have shown the effects of Stefan number and interface velocity on solidification processes in the numerical computations. The current results indicate that the inverse formulation is suitable for applications to problems over a range of Stefan numbers and interface velocity conditions. Further studies of inverse solidification problems can lead to automated control of various industrial processes, whereby the boundary temperature can be used to control the interface shape and motion, as well as various properties of the solidifying crystals and dendrites.

Appendix: Derivation of Eq. (14)

Equation (14) will be checked as follows. The starting point is the piecewise linear equation of state, Eq. (10), that is,

$$e = e_{r,k}(T) + c_{r,k}(T)(T - T_{r,k}) \tag{A1}$$

Using $T_{r,1} = 0$ (dimensionless) and $c_{r,1} = c_s/c_l$ in the solid phase, Eq. (A1) gives $e_s = c_s T_s/c_l$ in the solid when it approaches the phase-change temperature.

Then, following phase change into the liquid phase, the Gibbs equation is integrated from the solid s to liquid l phase as follows:

$$\int_s^l \mathrm{d}e = \int_s^l c_p \,\mathrm{d}T + \int_s^l L \,\mathrm{d}\lambda \tag{A2}$$

where c_p, L, and λ refer to the specific heat, latent heat of fusion, and liquid mass fraction, respectively. A linear variation of liquid fraction with temperature is assumed, that is,

$$\lambda = \frac{T - T_s}{T_l - T_s} \tag{A3}$$

For a pure material $(T_l - T_s) \approx \epsilon$, which represents a small value (typically of order 10^{-3}), because phase transition occurs over a negligibly small temperature range. A finite temperature range is still required in the numerical computations. However, for a binary constituent material T_l and T_s represent the liquidus and solid temperatures, respectively.

Substituting Eq. (A3) into Eq. (A2) and integrating results in

$$\int_s^l \mathrm{d}e = \frac{1}{2}(c_l + c_s)(T_l - T_s) + L \tag{A4}$$

After dividing by $c_l \Delta T_0$ ($\Delta T_0 = T_i - T_w$), substituting the earlier result for $e_s = c_s T_s/c_l$, and redefining $c_l \Delta T_0/L = Ste$ (Stefan number), the desired result in Eq. (14) is obtained.

Acknowledgment

Financial support from the Natural Sciences and Engineering Research Council of Canada for this research is gratefully acknowledged.

References

[1]Demirci, H. H., Coulter, J. P., and Guceri, S. I., "A Numerical and Experimental Investigation of Neural Network-Based Intelligent Control of Molding Processes," *Journal of Manufacturing Science and Engineering*, Vol. 119, Feb. 1997, pp. 88–94.

[2]Hale, S. W., Keyhani, M., and Frankel, J. I., "Design and Control of Interfacial Temperature Gradients in Solidification," *International Journal of Heat and Mass Transfer*, Vol. 43, No. 20, 2000, pp. 3795–3810.

[3]Minkowycz, W. J., Sparrow, E. M., Schneider, G. E., and Pletcher, R. H., *Handbook of Numerical Heat Transfer*, Wiley, New York, 1988.

[4]Trujillo, D. M., and Busby, H. R., *Practical Inverse Analysis in Engineering*, CRC Press, Boca Raton, FL, 1997.

[5]Beck, J. V., and Blackwell, B., "Inverse Problems," *Handbook of Numerical Heat Transfer*, edited by W. J. Minkowycz, E. M. Sparrow, G. E. Schneider, and R. H. Pletcher, Wiley, New York, 1988, Chap. 19.

[6]Tikhonov, A. N., and Arsenin, V. Y., *Solutions of Ill-Posed Problems*, V. H. Winston and Sons, Washington, DC, 1977.

[7]Bass, B. R., "Application of the Finite Element Method to the Nonlinear Inverse Heat Transfer Problem Using Beck's Second Method," *Journal of Engineering for Industry*, Vol. 102, No. 2, 1980, pp. 168–176.

[8]Osman, A. M., and Beck, J. V., "Nonlinear Inverse Problem for the Estimation of Time and Space Dependent Heat Transfer Coefficients," *Journal of Thermophysics and Heat Transfer*, Vol. 3, No. 2, 1989, pp. 146–152.

[9]Zabaras, N., "Inverse Finite Element Techniques for the Analysis of Solidification Processes," *International Journal For Numerical Methods in Engineering*, Vol. 29, No. 7, 1990, pp. 1569–1587.

[10]Katz, M. A., and Rubinsky, B., "An Inverse Finite Element Technique to Determine the Change of Phase Interface Location in One Dimensional Melting Problems," *Numerical Heat Transfer*, Vol. 7, No. 3, 1984, pp. 269–283.

[11]Zabaras, N., and Mukherjee, S., "An Analysis Solidification Problems by the Boundary Element Method," *International Journal for Numerical Methods in Engineering*, Vol. 24, No. 10, 1987, pp. 1879–1900.

[12]Zabaras, N., Mukherjee, S., and Richmond, O., "An Analysis of Inverse Heat Transfer Problems with Phase Changes Using an Integral Method," *Journal of Heat Transfer*, Vol. 110, No. 3, 1988, pp. 554–561.

[13]Voller, V. R., "Enthalpy Method for Inverse Stefan Problem," *Numerical Heat Transfer, Part B*, Vol. 21, No. 1, 1992, pp. 41–55.

[14]Voller, V. R., and Swaminathan, C. R., "Fixed Grid Technique for Phase Change Problems: A Review," *International Journal for Numerical Method in Engineering*, Vol. 30, No. 4, 1990, pp. 875–898.

[15]Patankar, S. V., *Numerical Heat Transfer and Fluid Flow*, Hemisphere, New York, 1980, Chaps. 3, 4, 7.

[16]Naterer, G. F., and Schneider, G. E., "PHASES Model of Binary Constituent Solid-Liquid Phase Transition—Part 1. Numerical Method," *Numerical Heat Transfer, Part B*, Vol. 28, No. 2, 1995, pp. 111–126.

[17]Xu, R., and Naterer, G. F., "Inverse Method with Heat and Entropy Transport in Solidification Processing of Materials," *Journal of Materials Processing Technology*, Vol. 112, No. 1, 2001, pp. 98–108.

[18]Carslaw, H. S., and Jaeger, J. C., *Conduction of Heat in Solids*, 2nd ed., Oxford Univ. Press, Oxford, 1959, Chap. 11.

[19]Chicatelli, A., Hartley, T., Cole, G., and Melcher, K., "Interdisciplinary Modelling Using Computational Fluid Dynamics and Control Theory," *Proceedings of the American Control Conference*, Baltimore, MD, 1994, pp. 3438–3443.

[20]Xu, R., "Control of Heat and Fluid Flow in Solidification Processes by an Inverse Method," M.S. Thesis, Dept. of Mechanical Engineering, Lakehead Univ., Thunder Bay, Canada, Dec. 1999.

[21]Krutz, G. W., "Application of the Finite Element Method to the Inverse Heat Conduction Problem," *Numerical Heat Transfer*, Vol. 1, 1978, pp. 489–498.

[22]Busby, H. R., and Trujllo, D. M., "Numerical Solution to a Two-Dimensional Inverse Heat Conduction Problem," *International Journal for Numerical Methods in Engineering*, Vol. 21, No. 2, 1985, pp. 349–359.

[23]Moutsoglou, A., "An Inverse Convection Problem," *Journal of Heat Transfer*, Vol. 111, No. 1, 1989, pp. 37–43.

[24]Reinhardt, H. J., "A Numerical Method for the Solution of Two-Dimensional Inverse Heat Conduction Problems," *International Journal for Numerical Methods in Engineering*, Vol. 32, No. 2, 1991, pp. 363–383.

[25]Maillet, D., Degiovanni, A., and Pasquetti, R., "Inverse Heat Conduction Applied to the Measurement of Heat Transfer Coefficient on a Cylinder: Comparison Between an Analytical and a Boundary Element Technique," *Journal of Heat Transfer*, Vol. 113, No. 3, 1991, pp. 549–557.

[26]Moulin, H. C., and Bayo, E., "Well-Conditioned Numerical Method for the Nonlinear Inverse Heat Conduction Problem," *Numerical Heat Transfer Part B*, Vol. 22, No. 3, 1992, pp. 321–347.

[27]Kang, S., and Zabaras, N., "Control of the Freezing Interface Motion in Two-Dimensional Solidification Processes Using the Adjoint Method," *International Journal for Numerical Methods in Engineering*, Vol. 38, No. 1, 1995, pp. 63–80.

[28]Li, Z. R., Prud'homme, M., and Nguyen, T. H., "A Numerical Solution for the Inverse Natural Convection Problem," *Numerical Heat Transfer Part B*, Vol. 28, No. 3, 1995, pp. 307–321.

[29]Frankel, J. I., and Keyhani, M., "A New Approach for Solving Inverse Solidification Design Problem," *Numerical Heat Transfer Part B*, Vol. 30, No. 2, 1996, pp. 161–177.

[30]Dorai, G. A., and Tortorelli, D. A., "Transient Inverse Heat Conduction Problem Solutions via Newton's Method," *International Journal of Heat and Mass Transfer*, Vol. 40, No. 17, 1997, pp. 4115–4127.